RESEARCH PAPER

The Effect of Anorthite on the Physical and the Mechanical Properties of Bone China Bodies

Zahra Rajabi Mashhadi*, Rahim Naghizadeh

* *zahra_rajabi_73@yahoo.com*

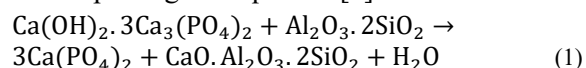School of Metallurgy and Materials Engineering, Iran University of Science and Technology, Tehran, Iran.

Abstract: Beta-tricalcium phosphate (β-TCP) and anorthite are the main crystalline components in bone china bodies. The difference in their thermal expansion coefficients causes a decrease in the thermal shock resistance of the body. In this study, anorthite was replaced with bone ash in the bone china body, and the effect of this change was studied on different properties of bone china after sintering at 1260°C for 3 h. The results showed that the physical and mechanical properties of the sample containing 50 wt.% anorthite compared to the typical bone china was improved and only 8.7% of the whiteness index was lost in this process. Also, the microstructure of anorthite samples, studied with SEM, showed no thermal cracks and revealed a uniform distribution of crystalline phase in the heterogeneous glass matrix.
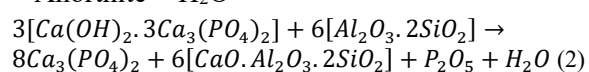
Keywords: Bone China Bodies, Anorthite, Thermal expansion coefficient, Thermal Cracks.

1. INTRODUCTION

Bone china is a new triple body that contains bone ash. Bone china bodies usually contain 50 wt% bone ash, 25 wt% clay, and 25 wt% feldspar [1]. What is happening in bone china sintering is very complex, and the mechanism of its reaction is still under discussion. In general, there are two main hypotheses were proposed by Beech and Robert about the sintering reaction between bone ash and kaolin: 1-NonPhosphate glass equation and 2-Phosphate glass equation [2].

$$Ca(OH)_2.3Ca_3(PO_4)_2 + Al_2O_3.2SiO_2 \rightarrow$$
$$3Ca(PO_4)_2 + CaO.Al_2O_3.2SiO_2 + H_2O \qquad (1)$$

Hydroxy apatite (Bone ash) + kaoline → β-TCP + Anorthite + H$_2$O

$$3[Ca(OH)_2.3Ca_3(PO_4)_2] + 6[Al_2O_3.2SiO_2] \rightarrow$$
$$8Ca_3(PO_4)_2 + 6[CaO.Al_2O_3.2SiO_2] + P_2O_5 + H_2O \quad (2)$$

Hydroxy apatite (Bone ash) + kaoline → β-TCP + Anorthite + P$_2$O$_5$ + H$_2$O

By sintering at 1250°C, both of these reactions result the formation of beta-tricalcium phosphate (β-TCP) and anorthite crystals in a heterogeneous glass matrix [3]. The specific feature of bone china that show its appeal are high strength, high glaze quality, whiteness and translucency. The last mentioned property results from the low refractive index difference of the crystalline phases with the glass and the small dimensions of the crystals. The presence of these fascinating features together in bone china makes it one of the most attractive and expensive types of cutlery in the world [4, 5].

Production of bone china bodies have problems both in preparing natural bone ash and in forming and sintering such as high sensitivity of bone ash behavior to preparation, low plasticity, and narrow firing temperature range. One of the main constraint in producing this body is the precise control of the firing temperature due to the narrow vitrification temperature range [5, 6]. More precisely, if the temperature rises slightly during synthesis, the body deforms. On the other hand, if the temperature decrease awhile, the crystal size of body component decreases and the amount of porosity increases. This will reduce the specific properties of bone china such as translucency and mechanical strength [5-8].

Due to the sharp difference of thermal expansion coefficient of β-TCP (12×10^{-6} K^{-1}) with other components, the possibility of thermal cracks in these bodies is very high. So, many efforts have been made to replace it with anorthite [9]. Anorthite (CaO.Al$_2$O$_3$.2SiO$_2$ or CAS$_2$) is used in most ceramic and glass ceramics bodies with low thermal expansion coefficient of 4.5×10^{-6} K^{-1}. The crystallization of anorthite improves physical properties of ceramic bodies, such as low thermal expansion coefficient, high thermal shock resistance and low dielectric constant. Also, formation of anorthite increases the strength and chemical stability of this triple bodies [10].

Zahra Rajabi Mashhadi, Rahim Naghizadeh

Because of the deficiency of anorthite with the purity accepted by industry in nature, its synthesis is performed in a variety of ways, most of which are based on the reaction of raw materials containing calcium carbonate and kaolinite. At the beginning of the synthesis there may be a large amount of gehlenite (Ca_2Al [$AlSiO_7$]), and mullite ($3Al_2O_3 \cdot 2SiO_2$) in body, but in the course of the synthesis process they change to anorthite [6].

The reactions in bone china bodies up to 1000°C are similar to those that happen in earthenware. The characteristic reactions of the bone china body accrue above this temperature [11]. Full mixing, adequate synthesis temperature, and phosphate melt fluidity are very effective in accelerating bone china body reactions. Generally, the following reactions occur with increasing temperature during bone china synthesis [3, 10-15]:

• 500-600°C _ Clay dehydration and burning organic material,
• 800 °C _ Bone ash conversion to lime and β-TCP,
• ≥800°C _ Conversion of lime and clay into anorthite,
• ≥900°C _ Melting alkaline oxides and formation a liquid state in the matrix,
• ≥1100°C _ Quartz decomposition,
• ≥1300°C _ Quartz and Anorthite decomposition,
• ≥1400°C _ β-TCP decomposition,
• ≥1500°C _ Glass phase.

Therefore, the bone china body is cured at about 1250°C and the final phases at the end of the synthesis are listed in Table 1.

Anorthite as a secondary crystalline phase formed 28% of the bone china body composition, along with β-tricalcium phosphate, which is the main crystalline phase of the body. Due to the different properties of the anorthite, its role in the body can be described as follows:

• The linear, intertwined and very small (100 nm)

anorthite crystals in the microstructure increase the strength and improve the mechanical properties of the body.
• The thermal expansion coefficient of anorthite is much lower than that of β-tricalcium phosphate and is closer to the thermal expansion coefficient of the glass phase. Therefore, the formation and increase of anorthite percentage in microstructure can reduce the thermal expansion coefficient of the whole body. The proximity of the thermal expansion coefficients of the phases to each other prevents the occurrence of thermal cracks and increases the thermal shock resistance of the body.
• Anorthite due to its low refractive index and its proximity to the glass phase can increase the translucency property in the body. Of course, the small dimensions of the anorthite crystals also contribute.
• Although the high melting point of the anorthite (1553°C) makes it difficult to solid-state sintering, but its replacement with bone ash in the raw material composition can prevent a sudden increase in melt volume during sinter. This, increases the vitrification temperature range and reduces the body deformation at the end of sinter.

In this study, for the first time, β-TCP formation in microstructure was entirely prevented by complete removal of bone ash from raw materials. Instead, synthesized anorthite, which was performed by mixing kaolin and calcite powders with a weight ratio of 7/3 at 1200°C for 3 h, was used in the body with various amounts of 10 to 50% by weight. The samples were subjected to different tests to investigate microstructural, physical and mechanical properties, thermal expansion coefficient, and whiteness index. The results showed that with the complete elimination of β-TCP phase, it is still possible to have a porcelain with the same bone china quality.

Table 1. Bone Chinese body composition after curing [1]

Phase	Chemical composition	Weight percent (wt %)	Thermal expansion coefficient ($\times 10^{-6}/_{°C}$)	Refractive index
β−TCP	$Ca_3(PO_4)_2$	43	12	1.63
Anorthite	$CaAl_2Si_2O_8$	28	4.3	1.573
Glass	$K_2O - Al_2O_3 - SiO_2 - CaO$	29	3-4.5	1.58

2. EXPERIMENTAL PROCEDURE

Traditional bone china body was made using a 2:1:1 ratio of bone ash, kaolin (%SiO_2:47.183, %Al_2O_3:35.85, %L.O.I:13.95) and potassium feldspar (%SiO_2:75, %Al_2O_3:13.1, %K_2O:6.75, %Na_2O:4.23, %L.O.I:0.28). Then, 10, 20 and 50 wt% of anorthite powder was used in this composition instead of bone ash powder. Table 2 shows the composition of the manufactured bodies and Figure 1 illustrates their manufacturing steps. To complete mixing and homogeneity, raw materials were milled into a jar mill containing alumina pellets and water for 3 h, and then passed through a sieve with 120 mesh number. The resulting slurry was heated for 24 h up to maximum temperature of 110°C with a rate of 10°C/min. In order to improve the reactivity and plasticity, powders' moisture was increased by 3% after grinding. After aging for 24 h, the powder was granulated to give a better press ability and passed through a 20-mesh sieve. Finally, the granular powder was pressed in to a mold (60×20×5 mm) under 30 MPa for 60 seconds. After shaping, the samples were dried at 110°C. To reduce the temperature gradient between surface and inside of samples and also to initiate sintering reactions, the samples were heated by a rate of 10°C/min up to 1000°C and kept at this temperature for 1 h Then, to complete the reactions of the bone china body, they reached 1260°C with the same rate, and were sintered at this temperature for 3 h.

Table 2. Composition of the manufactured bodies

Sample No	Anorthite (wt %)	Bone Ash (wt %)	Kaolin (wt %)	Potassium Feldspar (wt %)
A0	0	50	25	25
A10	10	40	25	25
A20	20	30	25	25
A50	50	0	25	25

Fig. 1. Manufacturing steps of the produced bodies

Zahra Rajabi Mashhadi, Rahim Naghizadeh

3. RESULTS AND DISCUSSIONS

3.1. DTA and TGA Analyses

DTA and TGA analyses of sample A50 were done up to 1400°C with a heating rate of 10°C/min in air atmosphere. According to this test, there is an endothermic peak in 570°C which is for thermal decomposition of kaolinite to metakaolin; and there are two exothermic peaks, one in 1000°C because of spinel Al-Si formation; and the other one in 1200°C because of anorthite deposition of eutectic melt. The reactions observed in thermal analysis of sample A50 containing 50 wt% anorthite, 25 wt% kaolin and 25 wt% potassium feldspar, are as follows:

Thermal decomposition of kaolinite to metakaolin;

$$Al_2O_3.2SiO_2.2H_2O \xrightarrow{570°C} Al_2O_3.2SiO_2 + 2H_2O \quad (3)$$
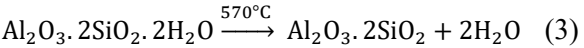
• Formation of spinel from metakaolin;

$$2(Al_2O_3.2SiO_2) \xrightarrow{1000°C} 2Al_2O_3.3SiO_2 + SiO_2 \quad (4)$$
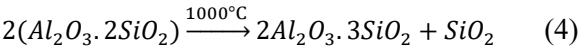
Figure 2 shows these reactions in DTA and TGA analysis of A50 samples. There is an exothermic peak at 1200°C that may be related to specific bone china reactions according to Iqbal studies [3, 15]. Subsequently, the microstructure of the body will be formed by the formation of low-volume eutectic melt and the deposition of new anorthite from the resulting melt [3, 8, 15].

According to the chemical composition of the raw materials, the percentages of the constituents after calcination of the samples are given in Table 3.

As shown in the Table 3, alkaline oxides did not change with respect to the constant weight percentage of the feldspar used. However, as the percentage of anorthite in the samples increased, the amount of alumina and silica increased and the calcium oxide decreased.
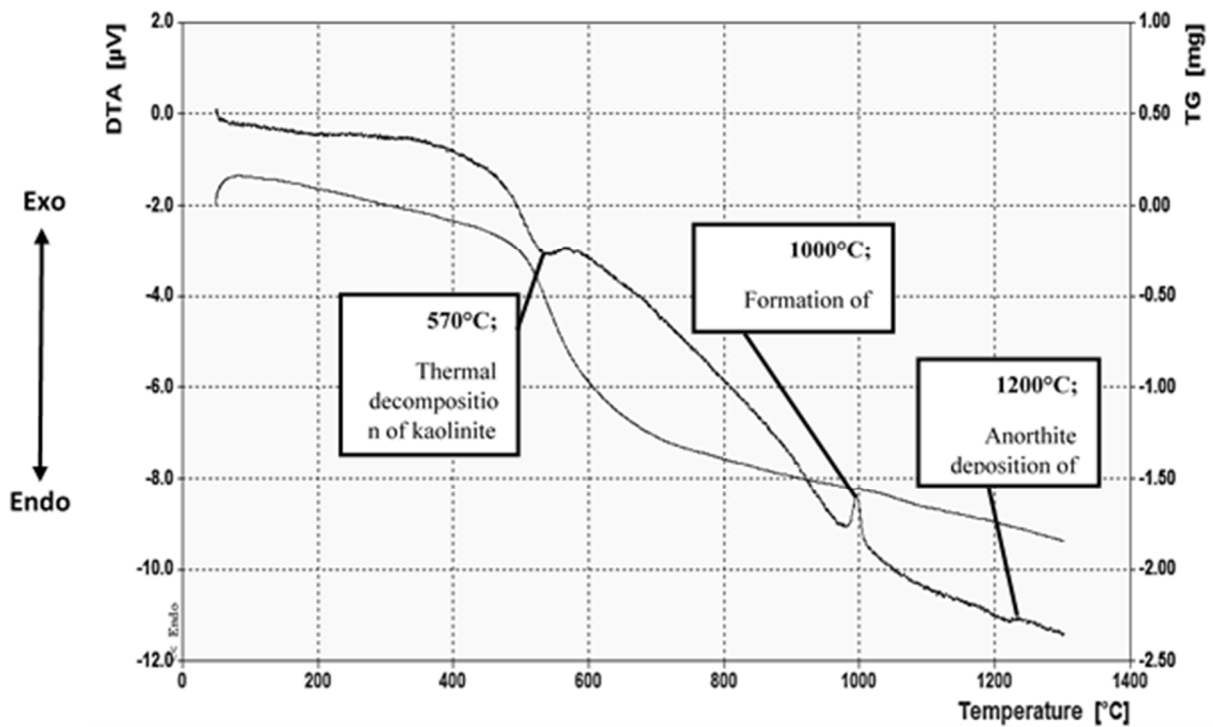

Fig. 2. DTA and TGA analyses for sample A50

Table 3. Chemical composition of samples A0, A10, A20 and A50 after calcination

Sample No	Chemical composition (wt %)							L.O.I (%)
	Al_2O_3	SiO_2	CaO	P_2O_5	K_2O	Na_2O	Other	
A0	13.16	30.38	27.96	19.20	1.69	1.06	0.03	4.45
A10	16.83	34.70	24.39	16.96	1.69	1.06	0.03	4.27
A20	20.49	39.01	20.83	12.72	1.69	1.06	0.03	4.09
A50	34.50	51.95	10.13	0	1.69	1.06	0.03	3.56

A50 sample contains the four major components of Al_2O_3, SiO_2, CaO and $K_2O + Na_2O$, and the weight percentages of them have undergone changes relative to the other samples. The important thing is the lack of phosphorus pentoxide which will lead to the lack of β-TCP phase in the body.

Table 3 shows the calculated loss on ignition (L.O.I) percentage for the A50 body is 3.56% and Figure 3 shows the weight loss of this sample by increasing the temperature up to 1400°C. According to this figure, about 3.5% weight loss is observed around 570°C due to the decomposition of kaolin to metakaolin.
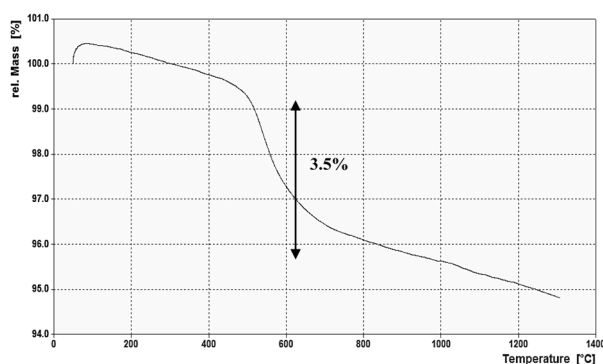

Fig. 3. Weight loss percent or L.O.I of A50 sample with increasing temperature

3.2. Phases Analysis

XRD results (Figure 4) demonstrated that there are three main crystalline phases of anorthite, β-TCP and Quartz in the sintered samples. As shown in Figure 4, by decreasing bone ash and increasing anorthite in the raw materials, the intensity of β-TCP main peak has been decreased and the intensity of anorthite main peak has increased. As long as the A50 body that has no bone ash, the peaks of the β-TCP phase are completely eliminated. In fact, the A50 sample is an almost anorthite body, and probably most of its microstructure consists of intertwined crystals of anorthite which be dispersed in glassy matrix.

According to experiments performed by Ptáček and Iqbal et al. [3, 10, 15], microstructural changes have been described during bone china body's heating. In sample A0, after structural evaporation, burning of organic matter, and decomposition of kaolinite to metakaolin, at 800°C, the hydroxyapatite in bone ash was decomposed into lime and crystalline phase of β-TCP. Near 900°C, the crystalline phase of anorthite was formed by the reaction of metakaolin with existing lime from the hydroxyapatite decomposition. It is also possible to form other calcium aluminosilicate phases such as Gehlenite. In the diffraction pattern of Figure 4, some peaks of these compounds are also identified. Up to temperatures above 1000°C, the low-melting eutectic composition of 9.5 K_2O - 10.9 Al_2O_3 - 79.8 SiO_2 is formed. As the temperature continues to rise, with the presence of potassium and sodium feldspars in the body, leucite ($KAlSi_2O_6$) is created around 1200°C. Due to the presence of silicate compounds in the body, dissolution of leucite occurred at a lower temperature than usual (1530°C) and it will be done at temperatures of 1200 to ultimately 1300°C. Other residual aluminosilicate compounds are also dissolved in the melt and finally, new anorthite will precipitate from existing calcium-rich aluminosilicate melt, which has high penetration rate. Upon completion of the curing and cooling the A0 sample, the microstructure consists of β-TCP, anorthite, gehlenite and quartz that are in the heterogeneous glassy matrix.

In samples A10 and A20, with the presence of anorthite in the composition of the body, this phase dissolves in the melt created and eventually, once the melt is saturated with aluminosilicate compounds, new anorthite will precipitate again from the melt. Increasing the weight percentage of anorthite in the primary composition of the body, increased the amount of new anorthite crystals and as shown in the diffraction pattern in Figure 4, the intensity of anorthite peaks increased in sample A20 compared to A10 and A0.

In sample A50, with the presence of anorthite instead of bone ash, raising the temperature up to 1050 °C along with the presence of potassium and sodium feldspars in the body cause sanidine formation with (NaK) $AlSiO_8$ formulation. However, the formation of sanidine does not occur in the presence of bone ash in the body (A0, A10 and A20). This flux phase will be molten at 1200°C. Under these conditions, the probability of dissolution of the existing anorthite in the melt will be increased and the amount of precipitation of new anorthite crystals will be increased, too. In the diffraction pattern, more new peaks of the anorthite have been identified, confirming this.
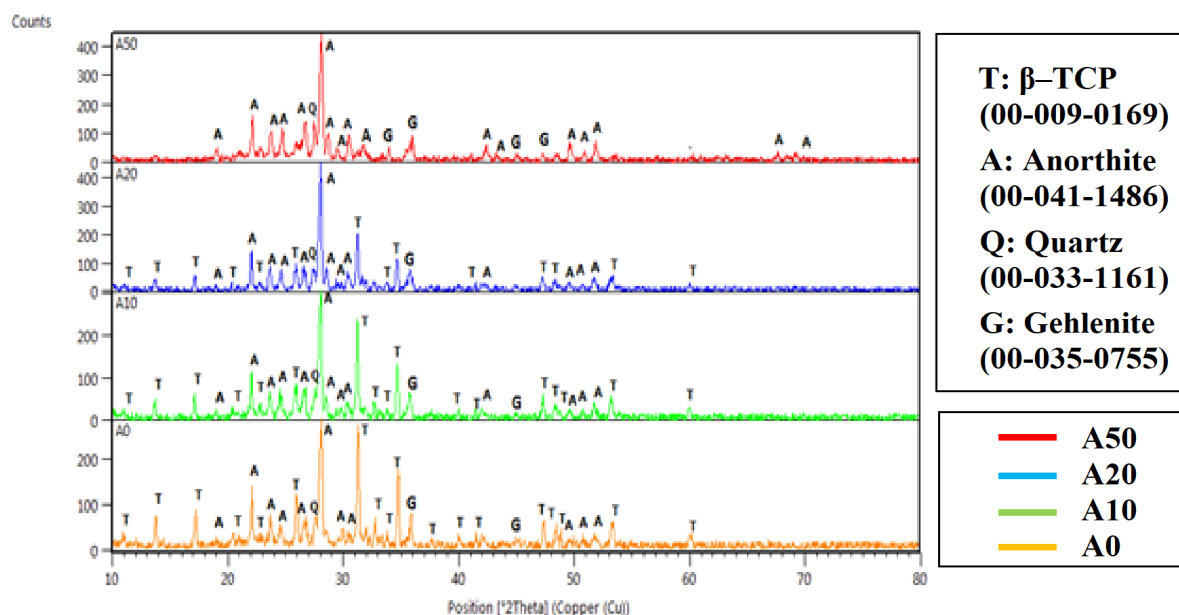
Fig. 4. Diffraction patterns (XRD) of samples with different weight percent of anorthite

Therefore, even if the metakaolin in this body became Al-Si spinel and later changed to mullite, in the presence of anorthite and existing feldspar, it will be gradually dissolved in the melt and new anorthite crystals will be precipitated from this melt. Finally, mullite and Al-Si spinels are not always detectable by XRD [16].

3.3. Microstructure and Morphology

Figure 5 shows the SEM images of the samples at 5000x magnification. In sample A0, a large number of β-TCP spherical particles are found alongside the intertwined particles of the anorthite. The very fine particles of anorthite and β-TCP (1 μm) have produced a relatively homogeneous microstructure. Micro-cracks caused by high thermal expansion coefficient of β-TCP are observed around these particles. In sample A10 the amount of β-TCP decreased and most of the microstructure contained anorthite particles of slightly larger size than sample A0. Reducing the percentage of bone ash in the composition of the body results a decrease in the percentage of flux phase in the sample and, as mentioned earlier, one of the roles of bone ash in bone china is to reduce the melting point of the body and improve the solid phase sintering. In addition to decreasing bone ash in these bone-anorthite bodies, the percentage of anorthite in the initial composition increased, which as a high melting point refractory material (about 1553°C)

would make it more difficult to sinter in solid state. This ensures that the sample sintering is not fully executed and porosity were enlarged in contrast to the A0 that were very small. In the sample A20, as in the A10, the percentage of decreased but the amount and size of the Anorthite and porosity increased. Thermal micro-cracks are still observed around the beta particles, although their size has decreased. The glassy phase percentage is also reduced by reducing bone ash, which is the main glass-forming phase in the body composition, and the small amount of phosphorus available only to create β-TCP phase. In some parts of the microstructures, the glassy phase is lost due to chemical etching of the sample with 5% HF and the cavity is observed. In sample A50, the microstructure lacks β-TCP and contains large and uniform anorthite particles along with coarse porosity. β-TCP removal reduces the coefficient of thermal expansion and no longer any micro-cracks due to the sharp difference of thermal expansion coefficients in the microstructure. This resulting in increased resistance to heat shock. Figure 6 shows the distribution of chemical composition in A0 and A50 samples (MAP analysis). Compare the distribution of chemical elements in this two sample indicates that by eliminating the bone ash from raw materials, the percentage of phosphorus element to zero, and this causes β-TCP phase is not formed.

6

Fig. 5. SEM images of the samples at 5000x magnification

Fig. 6. Distribution of chemical composition in samples A0 and A50 (MAP analysis)

Also in A50 sample due to dissolution of feldspar sanidine and melt formation, microstructure has more homogeneity than A0 sample. Because of the high penetration rate of calcium cation in the melt, anorthite deposition is possible in more parts of the body and the final microstructure will be approximately anorthite.

3.4. Physical and Mechanical Analysis

Density, water absorption and porosity percentage were calculated by Archimedes' Method, were calculated using the following equations [1]:

$$\rho_{bulk} = \frac{w_a}{w_b - w_c} \times \rho_{H_2O} \qquad (5)$$

$$\%Absorb = \frac{w_b - w_a}{w_a} \times 100 \qquad (6)$$

$$\%Porosity_{open} = \frac{w_b - w_a}{w_b - w_c} \times 100 \qquad (7)$$

In these equations, w_a is the sample mass in air, w_b is the sample mass submerged in water, and w_c is the mass saturated sample of water.

Generally, physical properties such as bulk density, water absorption and porosity percentage were improved by increasing the weight percentage of anorthite instead of bone ash in the studied bodies. The bulk density was reported for a standard bone china body 2.58 gcm^{-3} and for bone ash and anorthite, 1.3 and 2.76 gcm^{-3}, respectively [3, 15]. Therefore, replacement of bone ash with anorthite in raw materials leads to an increase in total density. On the other hand, the formation of the sanidine phase increases the melt and closes the open pores in the microstructure. Figure 7 shows that Density, water absorption and porosity percentage increase with increasing amount of anorthite in raw materials.

Fig. 7. Density, water absorption and porosity percentage changes with increasing amount of anorthite in raw materials.

As shown in Figure 8, bending strength of the samples increased significantly with increasing the weight percentage of anorthite in the raw material. This is due to the reduction of the micro-cracks caused by the sharp difference of the thermal expansion coefficients of the phases, the linear, intertwined and very small anorthite crystals in the microstructure.

Fig. 8. Changes in bending strength with increasing percentage of anorthite in raw materials.

3.5. Dilatometry Analyses

To determine the effect of anorthite on the thermal expansion coefficient of the body, dilatometry test was performed on samples A0 and A50. In this test, the changes in body length are calculated by increasing the temperature, and by the equation below, the slope of the relative length change curve in terms of temperature, determine the thermal expansion coefficient [1]:

$$\Delta L = L_0 \alpha \Delta T \qquad (8)$$

According to Figure 9, the thermal expansion coefficient of sample A0 was, on average, 8.876 $\times 10^{-6}$/°C and by replacing anorthite in A50 sample, this coefficient decreased by 40% to an average of 5.278 $\times 10^{-6}$/°C.

This decrease in the thermal expansion coefficient caused by the reduction of β-TCP can improve some of the bone china properties such as heat shock resistance and glaze scratch resistance. In fact, with the reduction and elimination of this phase in the body, the expansion coefficients of the other phases are in good agreement and due to thermal stresses, micro-cracks in the structure do not occur.

8

Fig. 9. Comparison of percentage changes in relative length of samples A0 and A50 with temperature.

3.6. Whiteness Analysis

Bone ash creates a clear white color, beauty and elegance of bone china bodies [16]. Since this product is used as a container and the beauty of this is very important, it should not be diminished in order to improve other properties such as strength and heat shock resistance. Thus, to investigate the effect of bone ash removal on the color of bone china body, the whiteness index of samples A0 and A50 were measured by using a spectrophotometer. According to Table 4, only 8.7% of the whiteness index of the body was reduced by completely removing bone ash from raw material. It can be said that this reduction can be neglected in order to dramatically improve other properties. As shown in Figure 10, which shows the color range in the C.I.E diagram, if the parameters a* and b* are closer to zero, the sample color is whiter.

Samples with negative a* and positive b* were in the green-yellow color range and samples with negative a* and b* are in the green-blue color range [16-18]. Thus, both samples are green-yellow in color, and fall within a range of C.I.E diagram. By reducing bone ash in the initial composition, the amount of pentoxide phosphorus in the body

is reduced, and therefore the body's whiteness index drops. Because phosphorus plays a key role in changing the capacity of iron impurity, which leads to a decrease in whiteness.
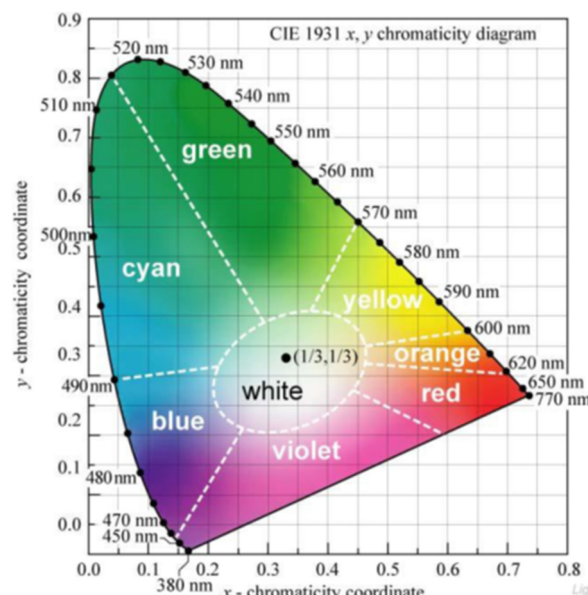

Fig. 10. C.I.E colour curve [13]

4. CONCLUSIONS

The results of this study can be summarized as follows:

1- The replacement of anorthite up to 50 %wt. by bone ash showed that the samples after sintering at 1260°C for 3 hrs had 0.79% porosity and 1.5% water absorption and bending strength of 68.9 MPa. Whereas the sample without anorthite had 5.54% open porosity and 8.04% water absorption and bending strength of 36.9 MPa.

2- By comparing the samples containing bone ash with those containing anorthite, it was observed that the micro-cracks resulting from the difference in thermal expansion coefficients of the phases are almost eliminated and also a more homogeneous microstructure is obtained.

Table 4. Whiteness index of samples A0 and A50

Sample No	WI-CIE	L^*	a^*	b^*	c^*	h^0
A0	70.16	90.37	-0.3	1.47	1.5	101.71
A50	64.4	88.95	-0.33	2.08	2.11	99.01

3- The thermal expansion coefficient was increased from 8.876 ×10^{-6}/°C in classic bone china sample to 5.278 ×10^{-6}/°C in the sample containing 50 wt. % Anorthite.

Complete removal of bone ash from bone china's raw materials reduced only 8.7% of the body whiteness index and changed it from 70.16 to 64.04.

ACKNOWLEDGEMENTS

REFERENCES

[1] Norton F. H., Fine ceramics: technology and applications, Part III, Kaolin, ed. McGraw-Hill Book Co. New York, USA, 1970, 260–415.

[2] Roberts, G. J., D. G. Beech, and D. Shen., "Glaze–body relationship in bonechina." Br. Ceram. Res., 1959, 18, 98-110.

[3] Iqbal, Y., P. F. Messer, and W. E. Lee., "Microstructural evolution in bone china." British ceramic transactions, 2000, 193-199.

[4] Ghosh R, Sarkar R., "Comparative Analysis of Novel Calcium Phosphate Based Machinable Bioceramic Composites." Transactions of the Indian Ceramic Society, 2020, 1-8.

[5] Kara A., Stevens R., "Characterisation of biscuit fired bone china body microstructure. Part I: XRD and SEM of crystalline phases." Journal of the European Ceramic Society, 2002, 22, 731-736.

[6] Kavalcı S., "The use of boron-containing additives for synthesis of anorthite ceramic powders." Master's thesis, Izmir Institute of Technology, 2006.

[7] Zhang J., Zhang Y., Wang K., Duan X., Hui C., and Wang Z.H., "The Influence of Holding Time on Morphologies and Electrochemical Properties of MAO/LDH Composite Film on LA103Z Mg-Li Alloy." Transactions of the Indian Ceramic Society, 2020, 79, 166-171.

[8] Weyl W.A., "Phosphates in ceramic ware: II, Role of phosphorus in bone china." Journal of the American Ceramic Society, 1941, 24, 245-247.

[9] Kara A., Stevens R., "Characterisation of biscuit fired bone china body microstructure. Part II: Transmission electron microscopy (TEM) of glassy matrix." Journal of the European Ceramic Society, 2002, 22, 737-743.

[10] Liao N., Jia D., Yang Z., and Li Y., "Enhanced Strengths and Thermal Shock Resistance of SiC-BN-10 Vol% Cf Composites through ZrB2 Addition." Transactions of the Indian Ceramic Society, 2019, 78, 204-211.

[11] Ptáček P., Opravil T., Šoukal F., Havlica J., and Holešinský R., "Kinetics and mechanism of formation of gehlenite, Al–Si spinel and anorthite from the mixture of kaolinite and calcite." Solid state sciences, 2013, 26, 53-58.

[12] Hortling A., Mannonen R., and Räsänen J., Bonechina of Lapland in Finland, Part I, ed. Book-Institue of Materials. New York, USA, 1999, 233–325.

[13] Pierre P.S., "Constitution of bone china: II, Reactions in bone china bodies." Journal of the american Ceramic Society, 1955, 38, 217-222.

[14] Kian K.M., "Reformulation of fine translucent porcelain." Doctoral dissertation, University of Sheffield, 2001.

[15] Iqbal Y., Messer P.F., and Lee W.E., "Non-equilibrium microstructure of bone china." British ceramic transactions, 2000, 99, 110-116.

[16] Zhang Y., Zhou N., Li W., Li J., Nian S., Li X., and Sui J., "Fabrication and characterization of bone china using synthetic bone powder as raw materials." Ceramics International, 2016, 42, 14910-14917.

[17] Kadyan S., Singh S., Sheoran S.,

Samantilleke A., Mari B., and Singh D., "Synthesis and Optoelectronic Characteristics of MGdAl$_3$O$_7$: Eu^{3+} Nanophosphors for Current Display Devices." Transactions of the Indian Ceramic Society, 2019, 78, 219-226.

[18] Prasad P.K., Reddy A.V., Rajesh P.K., Ponnambalam P., and Prakasan K., "Studies on rheology of ceramic inks and spread of ink droplets for direct ceramic ink jet printing." Journal of Materials Processing Technology, 2006, 176, 222-229.